

## CHAPTER V

### RESULTS

#### 1. Identification of the type of amino acid changes at the pr-M junction that affected the export of JEVpr/16681

In a previous study, the export of JEVpr/16681, a chimeric dengue serotype 2 virus containing a replacement with the 13-amino acid region just proximal to the pr-M cleavage site from JEV, out of infected PS cells was found to be delayed. The type and position of the amino acid replacement that affected the particle export were not yet known. In order to determine whether the changes in the three positively charged residues or the two negatively charged residues was responsible for the delayed virus export, the three pr-M junction mutant viruses generated by Songjaeng (2004) were used in the single-step kinetics studies.

##### 1.1 Viral propagation and nucleotide sequence analysis

Five dengue virus strains, including 16681Nde(+), JEVpr/16681, 16681pr(+7,-2), 16681pr(+4,-0)HS and 16681prE203A, were amplified in C6/36 cell line at 29°C for 5, 7 or 8 days and then subjected to focus immunoassay titration in order to determine the titer of infectious particles (Table 5). The mean titers derived from three separate titration attempts are shown in Table 5. Titers of more than  $1 \times 10^7$  FFU/ml were obtained with 16681Nde(+), 16681prE203A, 16681pr(+4,-0)HS and 16681pr(+7,-2). As reported previously, the maximum titer of JEVpr/16681 was only about  $1 \times 10^6$  FFU/ml on day 5 post infection (Keelapang et al., 2004). The presence of introduced mutations was confirmed by nucleotide sequence analysis of the semi-nested PCR products for all virus strains (Figure 8).

**Table 5.** Titer of dengue virus strains employed in the study.

Virus	Preparation	Day after Infection	Titer <sup>a</sup> (FFU/ml)
16681Nde(+)	C6-3(C6-2/3, D5, 22 Jan 04)	5	$1.08 \times 10^6$
		7	$6.27 \times 10^7$
JEVpr/16681	C6-3(C6-2, D5, 1 Jan 04)	5	$1.38 \times 10^6$
		8	$5.36 \times 10^5$
16681prE203A #1.1-10.1	C6-3/1(C6-2, D5, 26 May 05)	5	$3.78 \times 10^6$
		7	$3.42 \times 10^7$
16681pr(+4,-0)HS #5.4.11	C6-3(C6-2, D4, 20 Dec 03)	5	$6.48 \times 10^5$
		7	$1.65 \times 10^7$
16681pr(+7,-2)# 4.4-2.1	C6-3(C6-2, D4, 20 Dec 03)	5	$1.05 \times 10^5$
		7	$1.32 \times 10^7$

a, Data represent the arithmetic means derived from three separate titration attempts.

## 1.2 Determination of the levels of pr-M cleavage of three pr-M junction mutant dengue viruses

In an assessment of the changes in the level of prM cleavage, the three pr-M junction mutants and the chimeric virus, JEVpr/16681, were compared with the parent strain, 16681Nde(+). C6/36 cells were infected with these viruses and then radiolabeled at 48 h after infection for additional 18 hrs. Culture supernatants containing virus particles were subjected to PEG precipitation. The precipitates were resuspended with TES (pH 7.0) and the viral particles were partially purified by an isopycnic centrifugation using a 5-55% (w/v) sucrose gradient. The separated particles were removed with an upward displacement method into 15 equal fractions. The relative quantities of labeled proteins were next examined by dotting 2  $\mu$ l of these fractions.



onto a glass fiber filter paper and detecting the radioactivity signal by using a scintillation counter (Table 6). The three fractions, #2-6 (or #5-7 in an exceptional case of JEVpr/16681), which were expected to contain viral particles, were pooled and approximately 10,000 cpm of each virus pool were separated by 15% (w/v) SDS-PAGE. The gel was fixed, dried and exposed to a phosphorimager screen for two months (Figure 9). The screen was scanned with a phosphorimager and the viral protein bands corresponding to dengue E, prM and M proteins were identified. The intensity of the E band of about 55 kDa in lanes 3-7 appeared to be similar, indicating that these lanes contained an approximately equal amount of viral particles. Since the total numbers of E molecules and that of prM plus M on a single wild-type dengue virus particle are equal, i.e. 180 molecules/virion (Rice et al., 2001), the ratio of the signal (after an adjustment for the different quantities of cysteine and methionine) of E and (prM plus M) is expected to be 1.0. When the intensity of the E, prM and M protein bands of the parent virus and mutant viruses was determined and adjusted for the differences in the methionine-plus-cysteine content, it was found that the ratio of E/(prM plus M) signals of these viruses was between 1.05 to 1.45, consistent with the equimolar relationship between E and prM-plus-M.

In contrast to the similarity of the E band intensity observed among the virus strains, it was evident that the intensity of their prM bands was quite different. As compared with the parent strain, reduction of the prM band intensity was observed with 16681pr(+4,-0)HS, 16681pr(+7,-0) and JEVpr/16681 but not 16681pr(+7,-2) (Figure 9), indicating a greater level of prM cleavage in two of the three pr-M junction mutant viruses. In the three virus strains with reduced intensity of the prM band, there was a corresponding increase in the intensity of the M band. When the adjusted intensity signal of the prM and M bands were employed in the calculation of prM cleavage efficiency, it was found that the efficiency of prM cleavage in the parent strain 16681Nde(+) (62.5%) and the chimeric virus JEVpr/16681 (94.3%) was comparable to those previously determined by Keelapang et al (2004). For the two mutants with uncharged residues at P3 and P7, 16681pr(+4,-0)HS and 16681pr(+7,-0), the prM cleavage was detected at enhanced levels of 93.2% and 95.5%, respectively, which were in the same range with JEVpr/16681. On the other hand, the level of prM cleavage exhibited by 16681pr(+7,-2) was 67.2%, which was the same

level as the parent strain (Table 7). These results suggested that enhancement of prM cleavage in JEVpr/16681 was a consequence of the substitutions of negatively charged residues at P3 and/or P7 with uncharged amino acids. Substitution of the uncharged residues at P8, P10 and P13 with positively charged residue did not appear to affect prM cleavage.

**Table 6.** Total radioactivity in each fraction obtained from 5-55% sucrose gradient separation

Fraction Number	Radioactivity (cpm)				
	16681Nde(+)	16681pr(+7,-2)	JEVpr/16681	16681pr(+7,-0)	16681pr(+4,-0)HS
1	163	439	692	1067	93
2	137	163	1,261	1038	71
3	4,918	829	844	486	1,064
4	5,966	3,005	701	175	2,007
5	3,179	3,627	3,692	268	789
6	1,356	883	3,123	2,065	913
7	1,337	766	7,917	1,505	401
8	1,582	1,482	5,021	6,480	1,234
9	980	732	2,029	2,135	539
10	1,988	1,558	3,082	1,910	737
11	2,222	1,585	3,195	2,270	1,081
12	1,730	909	3,635	1,673	1,459
13	2,238	1,331	5,747	2,602	1,520
14	2,665	1,645	7,417	4,202	2,091
15	3,081	1,736	8,315	5,278	2,440



**Figure 9.** Analysis of sucrose gradient - purified viral particles. Virus-infected C6/36 cells were labeled with  $^{35}\text{S}$ -methionine and  $^{35}\text{S}$ -cysteine for 18 hours. Virus particles in culture medium were concentrated with polyethylene glycol precipitation and partially purified by centrifugation in a 5-55% sucrose gradient. The fractions containing viral particles were pooled, lysed and separated with 15% SDS-PAGE. Labeled protein bands were detected by using a phosphoimager. Lanes 1-3 were loaded with 116,640, 11,664 or 1,166 cpm of 16681Nde(+). Lane 4, 16681pr(+4,-0)HS (7,623 cpm); lane 5, 16681pr(+7,-0) (13,590 cpm); lane 6, 16681pr(+7,-2)(7,560 cpm); lane 7, JEVpr/16681 (13,644 cpm).

**Table 7.** Efficiency of prM cleavage in dengue viruses.

Virus	E/(prM+M) ratio	Pr-M cleavage (%)	Total prM (molecule/virion)	Total M (molecule/virion)
16681Nde(+) (116,640 cpm)	1.05	66.2	60.9	119.1
16681Nde(+) (11,664 cpm)	1.38	63.6	65.5	114.5
16681Nde(+) (1,166 cpm)	1.22	62.5	67.5	112.5
16681pr(+4,- 0)HS (7,623 cpm)	1.21	93.2	12.3	167.7
16681pr(+7,- 0) (13,590 cpm)	1.18	95.5	8.2	171.8
16681pr(+7,- 2) (7,560 cpm)	1.40	67.2	58.9	121.1
JEVpr/16681 (13,644 cpm)	1.16	94.4	10.2	169.8

### 1.3 Determination of the type of amino acid changes at the pr-M junction that affected particle export

In the investigation of the structural basis for delayed virus export in the chimeric virus JEVpr/16681, a single-step kinetics replication studied was employed using PS cells. Confluent monolayers of the PS cell line, at approximately  $1.0 \times 10^6$  cell/dish, were infected with 16681Nde(+), JEVpr/16681, 16681pr(+7,-2),

16681pr(+4,-0)HS, and a single point mutant virus, 16681prE203A, at the MOI of 1. Culture media and infected cells were collected at 0, 4, 12, 14, 16, 20, 24, 36, 48 h post infection. For the quantitation of cell-associated viruses, infected cells were subjected to three consecutive cycles of freezing and thawing on ice to release viral particles from cells. Infectious virus titers of the extracellular and cell-associated viruses were then determined by using the focus immunoassay titration.

In the single-step kinetics experiment, changes in the titers of 16681 and JEVpr/16681 were consistent with the delay of virus export in JEVpr/16681 previously described by Keelapang et al. (2004)(Figure 10). The infectious titers of cell-associated viruses of JEVpr/16681 (and the other three pr-M junction mutants) were similar to those of the parent virus at all time points. In contrast, the titers of the extracellular viruses of JEVpr/16681 were always lower than those of 16681Nde(+) at any time after 12 h of the infection. Similar reductions of the extracellular infectious virus titer were observed with 16681pr(+7,-2), but not 16681pr(+4,-0)HS and 16681prE203A (Figure 10). Thus, the substitutions of uncharged residues at P8, P10 and P13 positions with arginine in 16681pr(+7,-2) were sufficient to cause the delayed virus export whereas the substitutions of the negatively charged residues at P3 and/or P7 with uncharged residues did not affect export.

These results demonstrated that the substitutions with positively charged amino acid substitutions at the cleavage positions P8, P10, and P13 were associated with a delay in the export of infectious virus particles in JEVpr/16681. In contrast, the substitution of the negatively charged residues at P3 and P7 with uncharged residues, despite of the clear enhancing effect on the pr-M cleavage efficiency, did not appear to affect particle export.

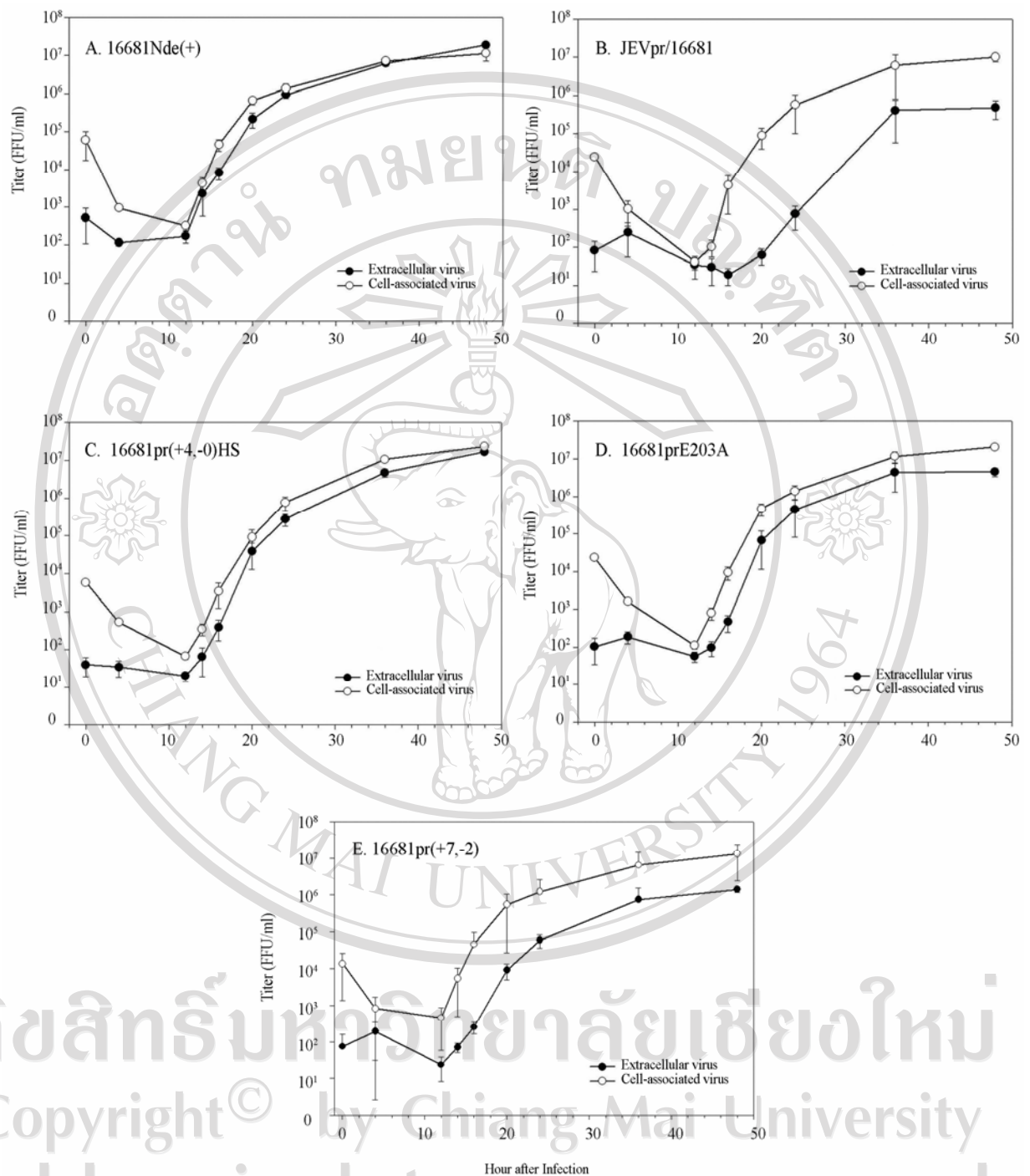


**Figure 10.** Single-step kinetics replication of the parent and the pr-M mutant viruses. Titters are means and standard deviation derived form 3 separated experiment. A, 16681Nde(+); B, JEVpr/16681; C, 16681prE203A; D, 16681pr(+4,-0)HS; E, 16681pr(+7,-2).

## **2. Identification of the amino acid(s) within the 13-amino acid region just proximal to the pr-M junction that affected particle export**

The reduction of extracellular infectious virus titers observed in 16681pr (+7,-2) suggested that substitution of uncharged amino acids at P8, P10 and P13 with arginine negatively affected the export of infectious virions of JEVpr/16681. It was not clear whether all three arginine residues were required to exert this effect, or a combination of two arginine residues, or even single arginine residue at one of these three positions, were sufficient. In an attempt to distinguish between these possibilities, three sets of double arginine substitution mutations were introduced into the pr-M cleavage junction of the full-length cDNA clones of dengue virus strain 16681Nde(+). Mutant viruses were then propagated in C6/36 cells and the intended mutations were verified by RT-PCR and nucleotide sequence analysis. The second set of infectious mutant viruses were then employed in the single-step replication kinetics study as described below.

### **2.1 Generation of three pr-M junction mutant dengue viruses**

Three sets of oligonucleotides were designed for the introduction of the following double point mutations into the genome of 16681Nde(+): pr(+6,-2)P10,13+ harboring threonine-to-arginine and threonine-to-arginine amino acid substitutions at P10 and P13; pr(+6,-2)P8,13+ harboring glycine-to-arginine and threonine-to-arginine amino acid substitutions at P8 and P13, and pr(+6,-2)P8,10+ harboring glycine-to-arginine and threonine-to-arginine amino acid substitutions at P8 and P10 (Table 2). For the ease in checking the presence of the introduced mutations, the restriction enzymes recognition sites were also incorporated into these oligonucleotides: BsrG I site in pr(+6,-2)P10,13+ and Sph I site in pr(+6,-2)P8,10+. The oligonucleotide were ligated into a plasmid subclone and the 1.3 kb fragment containing those mutation were subsequently transferred into the 5' half genome, pBK(S1SP6-4497). Ligation of the 5' half genome with a DNA fragment containing the region 4497-10723 of the viral genome generated the full-length cDNA clone with the desired double mutation.

The resultant mutant full-length cDNA clones were then used in the production of capped *in vitro* RNA transcripts and, subsequently, mutant progeny viruses.

### 2.1.1 Construction of pBK(S1SP6-1547) subclones carrying double mutations

A recombinant pBluescript II KS+ plasmid, which contained the region nt 1-1547 of dengue type 2 strain 16681 genome and two introduced restriction sites, Nde I site at nt 666 and BamH I site at nt 709, was constructed by Keelapang et al. (2004). The plasmid was digested with Nde I and BamH I, ligated with the double-stranded oligonucleotides with compatible cohesive ends, and then transformed into an *E.coli* strain, DH5 $\alpha$ F'. Transformed cells were selected with ampicillin and grown in a small scale culture. When the plasmid DNA preparation was analyzed by 0.7% agarose gel electrophoresis, the expected 4.5 kb supercoiled DNA band was observed (Figure 11). Five clones were selected for the identification of intended mutation by using appropriate restriction enzymes, i.e. BsrG I for pBK(S1SP6-1547)pr(+6,-2)P10,13+ and Sph I for pBK(S1SP6-1547)pr(+6,-2)P8,10+. For pBK(S1SP6-1547)pr(+6,-2)P10,13+ a single linear DNA band, about 4.5 kb in size, was expected. In the case of pBK(S1SP6-1547)pr(+6,-2)P8,10+, two bands of 3.6 kb and 0.7 kb in size were anticipated. Two clones were then grown at a larger volume of LB broth (100 ml) at 22.5°C for 2 days for each mutant recombinant subclone.

The midi-preparation of 4.5 kb subclone plasmids was analyzed by 0.7% agarose gel electrophoresis (Figure 11). The concentrations of the mutant subclone plasmids were: 189 ng/ $\mu$ l for pBK(S1SP6-1547)pr(+6,-2)P10,13+, 492.33 ng/ $\mu$ l for pBK(S1SP6-1547)pr(+6,-2)P8,10+ and 111.42 ng/ $\mu$ l for pBK(S1SP6-1547)pr(+6,-2)P10,13+. For pBK(S1SP6-1547)pr(+6,-2)P8,13+, the presence of the intended mutations was verified by DNA sequencing as the suitable restriction enzyme recognition site for rapid screening could not be found (Figure 12). The electropherogram of the sequencing reaction revealed that the subclone plasmid pBK(S1SP6-1547)pr(+6,-2)P8,13+ contained the desired double mutations at positions P8 and P13 as expected. Additional mutation was not detected in the entire prM coding region of this subclone.

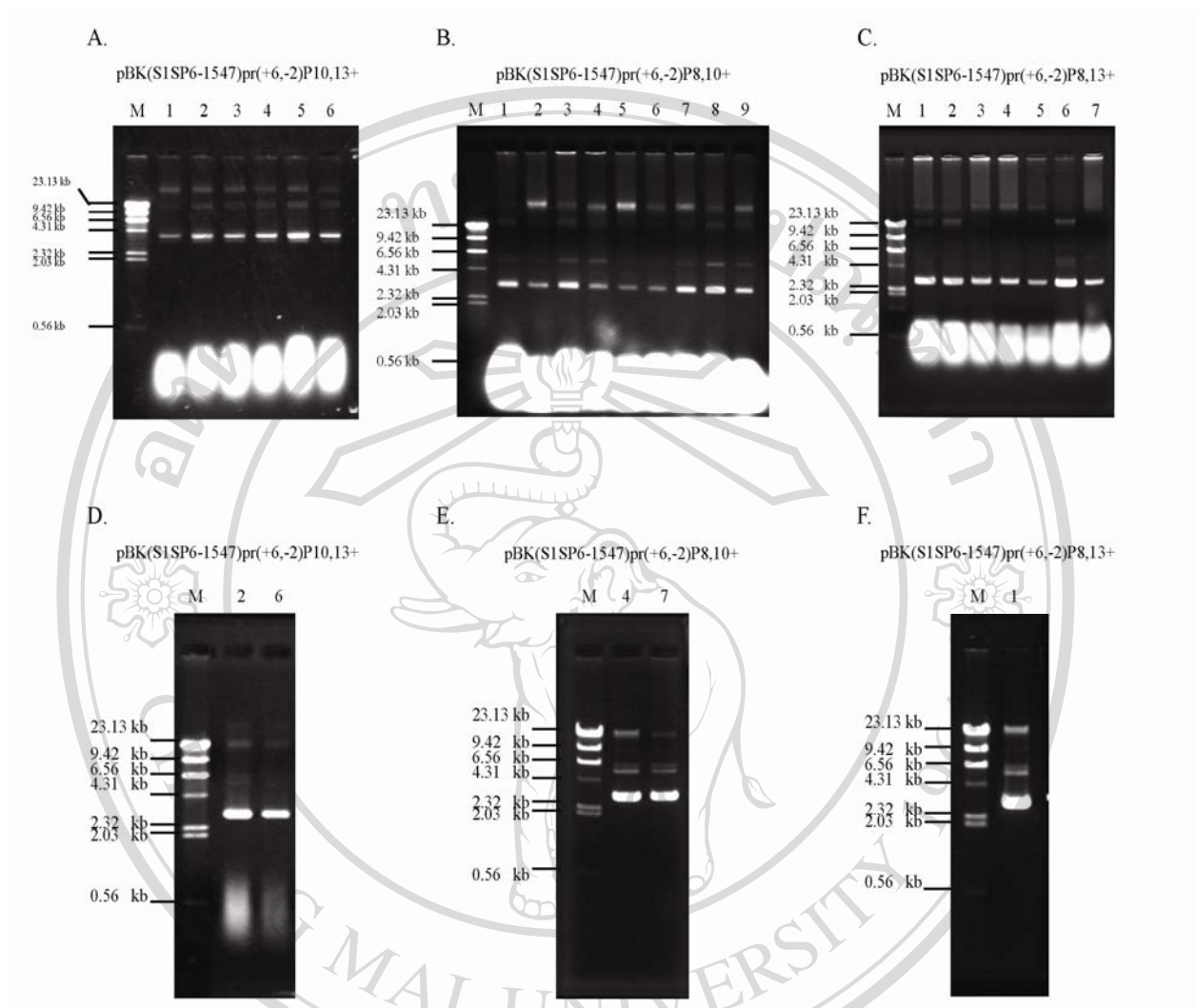


**Figure 11.** Analysis of DNA preparations by agarose gel electrophoresis. Mini (panel A-C) DNA preparation and midi (panel D-F) DNA preparations were separated in 0.7% agarose gel without prior restriction enzyme digestion. Panel A, pBK(S1SP6-1547)pr(+6,-2)P10,13+; B, pBK(S1SP6-1547)pr(+6,-2)P8,10+; C, pBK(S1SP6-1547)pr(+6,-2)P8,13+; D, pBK(S1SP6-1547)pr(+6,-2)P10,13+; E, pBK(S1SP6-1547)pr(+6,-2)P8,10+; F, pBK(S1SP6-1547)pr(+6,-2)P8,13+. The sizes in kb of the  $\lambda$  DNA digested by Hind III, lane M, are on the left, and the numbers above each panel represent clone designation.

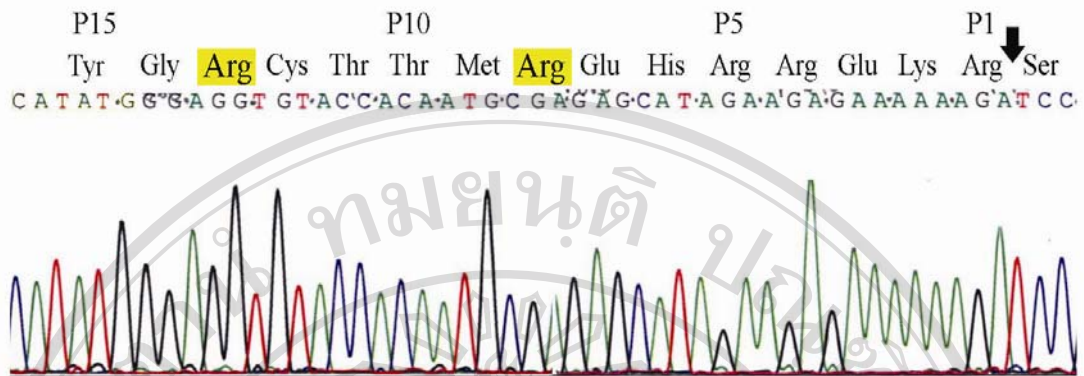


**Figure 12.** Nucleotide sequence analysis of pBK(S1SP6-1547)pr(+6,-2)P8,13+. The sequence of subclone plasmid was determined with the primer S350. The yellow highlighting-residues represented the desirable arginine substitutions. Only the pr-M junction sequence was shown. Arrow indicates the pr-M cleavage junction.

### 2.1.2 Construction of 5' half genome containing double mutations at the pr-M junction

Following the introduction of mutagenic oligonucleotides into the subclone plasmids, the 1.3 kb Pst I fragment containing the entire prM coding region with the desired double mutation at the pr-M junction was transferred to the 5' half genome. The mutant subclone plasmid was digested with Pst I yielding the two expected fragments of 3.2 kb and 1.3 kb in size. The 1.3 kb Pst I fragment was excised and purified by a gel extraction purification kit (Figure 13) and the quality of these purified fragments was analyzed with agarose gel electrophoresis. The concentration of the purified 1.3 kb Pst I fragment was: 100.00 ng/ $\mu$ l for pBK(S1SP6-1547)pr(+6,-2)P10,13+, 105.88 ng/ $\mu$ l for pBK(S1SP6-1547)pr(+6,-2)P8,10+ and 28.0 ng/ $\mu$ l for pBK(S1SP6-1547)pr(+6,-2)P8,13+.

The 5' half genome, pBK(S1SP6-4997), was digested with Pst I to completion, treated with CIAP to remove the terminal phosphate group and then purified. The large Pst I fragment, 6.0 kb in size, of the 5' half genome was then ligated with the 1.3 kb Pst I fragment derived from the mutant subclone plasmid. The resultant mutant 5' half genome plasmid was transformed into *E.coli*, plated on LB

agar containing 25 µg/ml ampicillin and incubated at 22.5°C for 2 days. Ten pinpoint smooth colonies were picked into 2 ml LB broth containing 25 µg/ml ampicillin and returned to incubation at 22.5°C with constant shaking for the preparation of plasmid DNA.

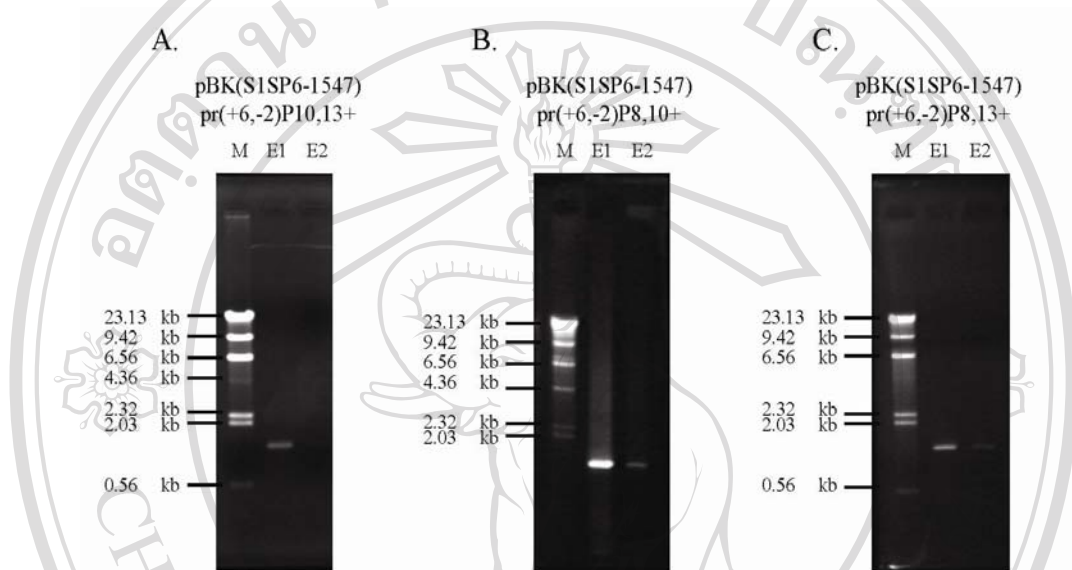


**Figure 13.** Purification of mutants 1.3 kb Pst I fragments: A, 1.3 kb fragment form pBK(S1SP6-1547)pr(+6,-2)P10,13+; B, 1.3 kb fragment form pBK(S1SP6-1547)pr(+6,-2)P8,10+, C, 1.3 kb fragment form pBK(S1SP6-1547)pr(+6,-2)P8,13+. E1 and E2 represent elution # 1 and elution # 2, respectively. The sizes in kb of the  $\lambda$  DNA Hind III-digested fragments, lane M, are on the left.

From this ligation, there were three possible outcomes: 1) self ligation between nt 212 and nt 1535 at the two Pst I-digested ends of pBK(S1SP6-4497), 2) insertion of the 1.3 kb Pst I fragment into pBK(S1SP6-4497) in an inverse orientation, and 3) insertion of the 1.3 kb Pst I fragment into pBK(S1SP6-4497) in the correct orientation. In an attempt to identify the mutant 5' half genome with the proper orientation, the mini plasmid preparations were doubly digested with EcoR I + Sph I as well as with BsrG I alone or Sph I alone.

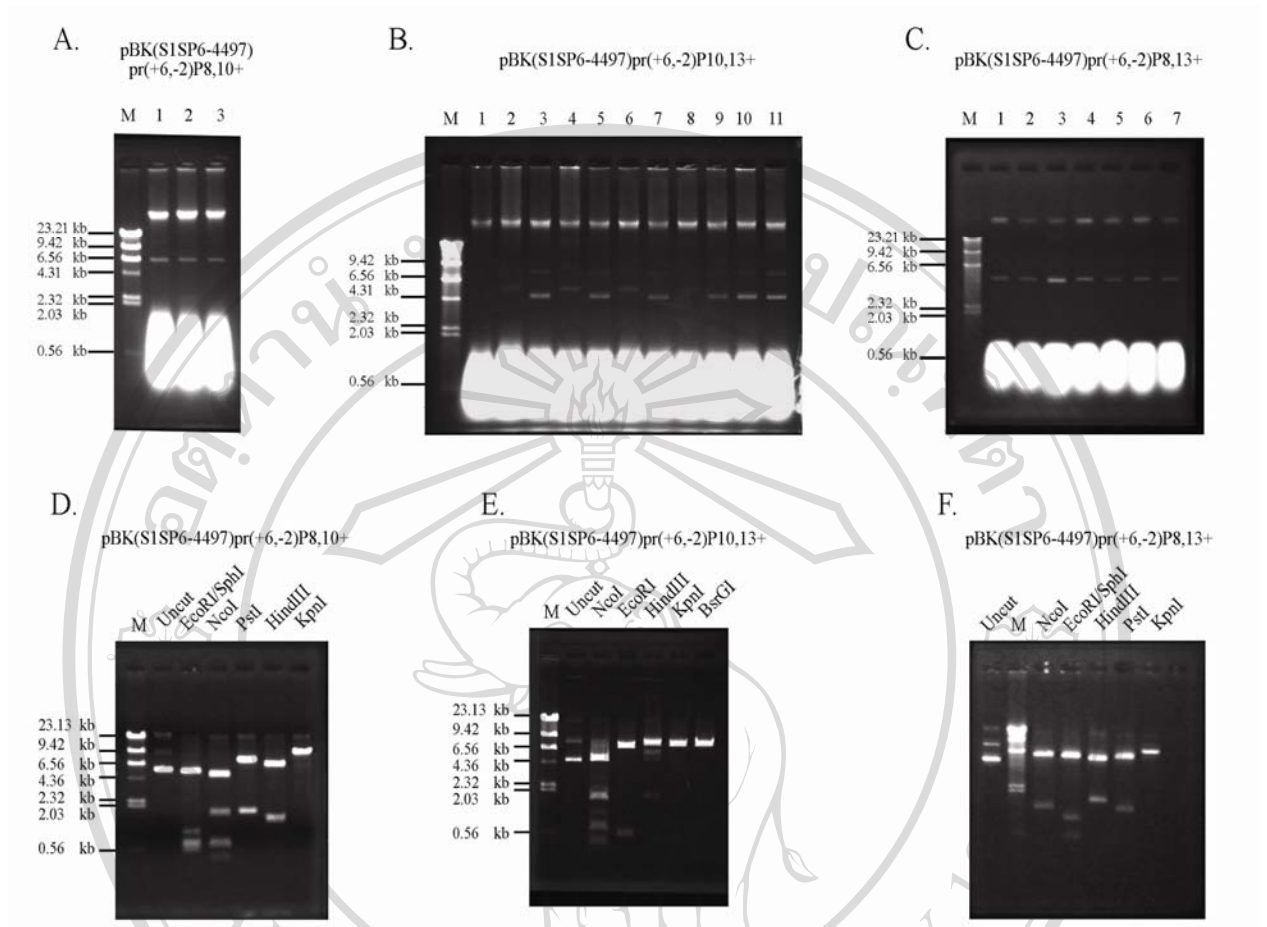


**Figure 14.** Mini-DNA preparation of mutant 5' half genome and restriction enzyme digestion analyses. A-C, mini-DNA preparation; A, pBK(S1SP6-4497)pr(+6,-2)P8,10+; B, pBK(S1SP6-4497)pr(+6,-2)P10,13+; C, pBK(S1SP6-4497)pr(+6,-2)P8,13+ and D-F, midi-DNA preparation of mutant 5' half genomes was digested with five set of restriction enzymes; D, pBK(S1SP6-4497)pr(+6,-2)P8,10+; E, pBK(S1SP6-4497)pr(+6,-2)P10,13+; F, pBK(S1SP6-4497)pr(+6,-2)P8,13+. The sizes in kb of the  $\lambda$  DNA Hind III-digested fragments are on the left. The clone designation is shown in numbers above each panel.

Following BsrG I digestion, the plasmid pBK(S1SP6-4497)pr(+6,-2)P10,13+ yielded an expected linear DNA band of approximately 7.3 kb in size. With the single Sph I digestion, pBK(S1SP6-4497)pr(+6,-2)P8,10+ yielded two bands of 6.7 kb and 0.69 kb in size. The mutant 5' half genome pBK(S1SP6-4497)pr(+6,-2)P8,10+ with an insertion in the correct orientation resulted in four bands of 5.21, 0.96, 0.69 and 0.53 kb in size after double digestion with EcoR I+Sph I whereas pBK(S1SP6-4497)pr(+6,-2)P10,13+ resulted in three bands of 3.03, 0.96 and 0.54 kb in size. Based on these results, two recombinant clones with insertion in the correct orientation were further inoculated into 100 ml of LB broth containing 25 µg/ml ampicillin and incubated at 22.5°C for 2-3 days with shaking. Cells were harvested by centrifugation and subjected to plasmids DNA midi-preparation. The mutant 5' half genomes were next digested with five sets of restriction enzymes to examine the distribution of the sites within these plasmid clones. Figure 14D-F revealed the expected DNA fragments of 0.37, 0.54, 1.63 and 4.73 kb following Nco I digestion; 1.32 and 6.08 kb following Pst I digestion; 1.69 and 5.71 kb following Hind III digestion; 6.87 and 0.53 kb following EcoR I digestion. The presence of intended double mutation in pBK(S1SP6-4497)pr(+6,-2)P10,13+ and pBK(S1SP6-4497)pr(+6,-2)P8,10+ were examined with BsrG I and Sph I digestions, respectively, and the expected single 7.3 kb BsrG I band and the two fragments of 6.70 and 0.7 kb in size were clearly detected in each case. The mutation in pBK(S1SP6-4497)pr(+6,-2)P8,13+ was again confirmed by nucleotide sequence determination (Figure 15).

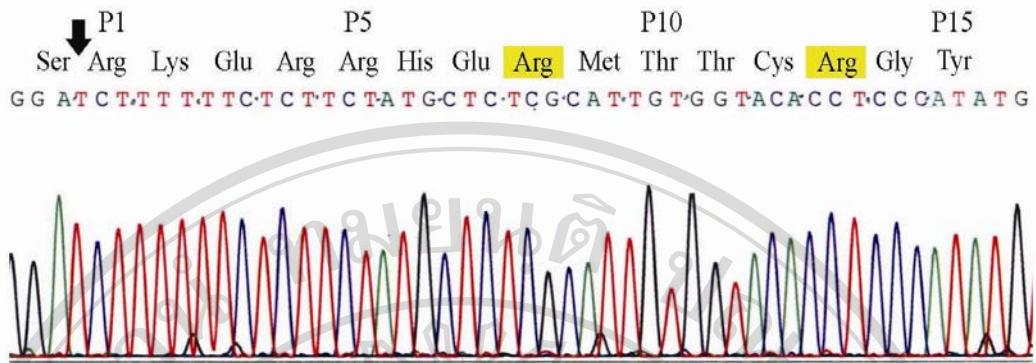


**Figure 15.** Nucleotide sequence analysis of the pr-M junction in pBK(S1SP6-4497)pr(+6,-2)P8,13+. The primer C859 was employed in the sequencing reaction. This sequence shown represents the non-coding strand, and the yellow highlighting-residues represent the intended arginine substitutions. Arrow indicates the pr-M junction.

### 2.1.3 Construction of the pr-M junction mutant full-length cDNA clones

In the generation of the full-length cDNA clones containing the desired mutation, 5 µg of the 7.3 kb 5' half genome was linearized with Kpn I digestion, treated with CIAP, ligated to the 3' half genome and then transformed into *E. coli* and selected with ampicillin as described previously. The 3' half genome fragment containing the dengue cDNA sequence nt 4498-10723 flanked by Kpn I recognition site was digested from pBK(4497-10723) with Kpn I. After three days of incubation at 22.5°C, bacterial colonies of three difference sizes observed: large, medium and pinpoint. Ten pinpoint colonies of transformants were picked into LB broth containing 25 µg/ml ampicillin and returned to incubation at 22.5°C with shaking for additional 3 days. Plasmid DNA mini-preparations of the bacterial transformants were analyzed with agarose gel electrophoresis (Figure 16A-B). The results revealed a variety of DNA bands. The clones that were in the ranges of 6.56-9.42 kb were selected for checking by restriction enzyme digestions. Identification of the orientation of the inserted 3' half genome sequence and confirmation of the intended double mutations were performed by digestions with Xba I/Hind III, and BsrG I or Sph I).

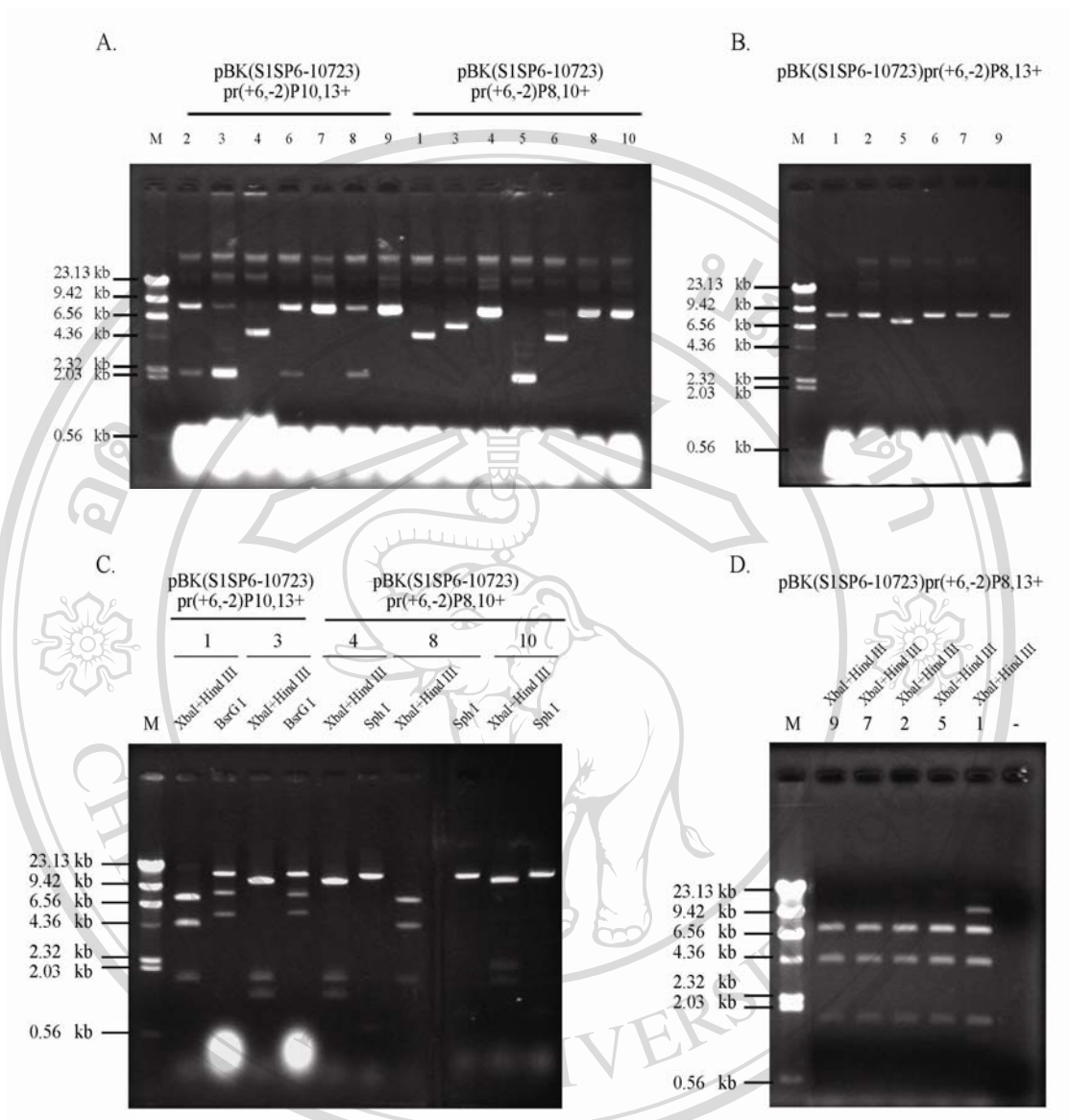


**Figure 16.** Agarose gel electrophoresis of plasmid DNA mini-preparations of the mutant full-length cDNA clones and screening by restriction enzyme digestion analyses. A, B, Plasmid DNA without restriction enzyme digestion. C, D, Identification of the orientation of the inserted 3' half genome sequence and the presence of intended mutations by restriction enzyme digestion (Xba I/Hind III, and BsrG I or Sph I). The sizes in kb of the  $\lambda$  DNA Hind III-digested fragments are on the left. Clone designation was shown as numbers above each panel.

Based on the screening results, two full-length cDNA clones were selected for a 100-ml scale culture under ampicillin selection. Subsequently, plasmid DNA

preparations were analyzed with agarose gel electrophoresis (Figure 17A-C). Also, 300 ng of the purified plasmid DNA were digested with five sets of restriction enzymes (Figure 17D-F).

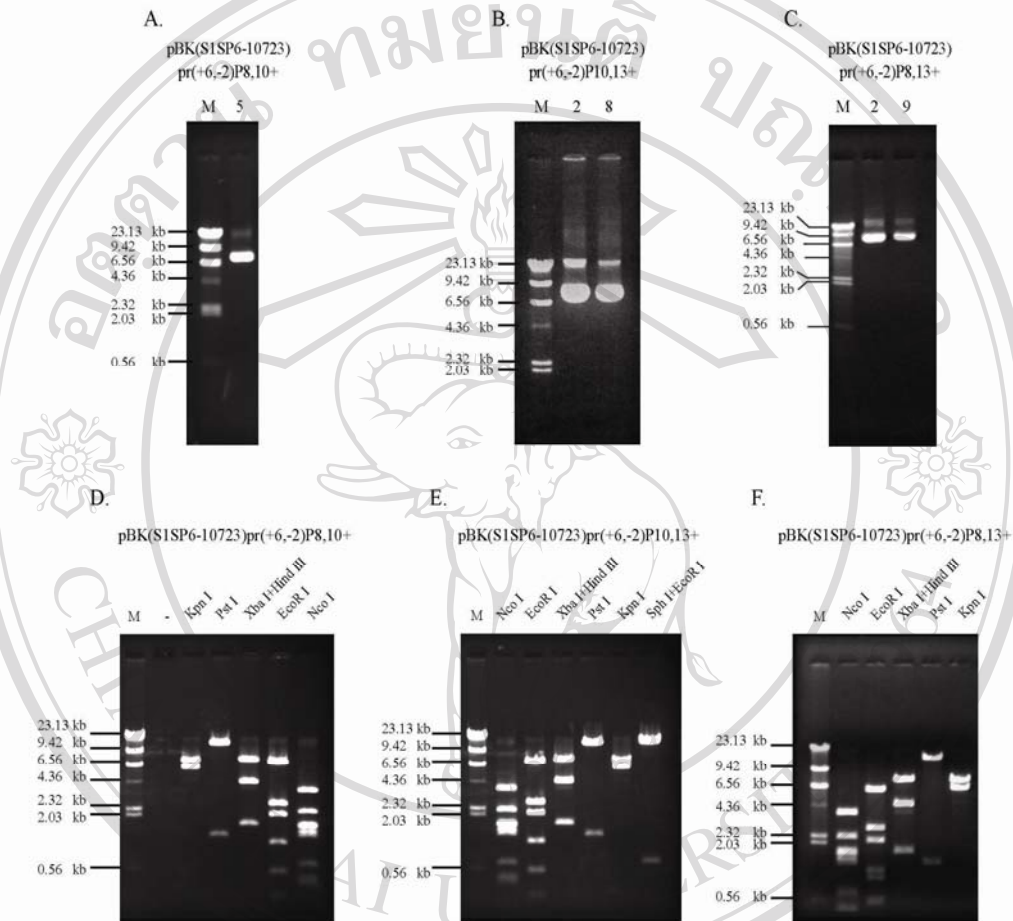


**Figure 17.** Midi-DNA preparation of double mutations full-length cDNA clones and restriction enzymes analyses. A-C, midi-DNA preparation without digestion: A, pBK(S1SP6-10723)pr(+6,-2)P8,10+; B, pBK(S1SP6-10723)pr(+6,-2)P10,13+; C, pBK(S1SP6-10723)pr(+6,-2)P8,13+. D-F, midi-DNA preparation was digested with 5 sets of restriction enzymes: D, pBK(S1SP6-10723)pr(+6,-2)P8,10+; E, pBK(S1SP6-10723)pr(+6,-2)P10,13+; F, pBK(S1SP6-10723)pr(+6,-2)P8,13+. The sizes in kb of the  $\lambda$  DNA Hind III-digested fragments are on the left. Clone designation was shown as numbers above each panel.



In this restriction enzyme analysis, all of the expected DNA fragments were observed: 12.94 and 0.70 kb fragments following Sph I digestion; 12.31 and 1.32 kb fragments following Pst I digestion; 8.00 and 6.23 kb fragments following Kpn I digestion; and 7.01, 2.68, 2.08 and 1.12 kb fragments following EcoR I digestion. The restriction enzyme digestion profiles revealed that there was no large scale deletion or insertion involving the fragments that were digested with the restriction enzymes employed. In the preparation of the *in vitro* RNA transcripts, one of the two clones was linearized by Xba I digestion (figure 19), purified and quantitated.

#### 2.1.4 Generation of capped *in vitro* transcripts

In the generation of infectious *in vitro* transcripts of the full-length mutant cDNA clones, one  $\mu\text{g}$  of the linearized mutant full-length cDNA clone was used as templates in the *in vitro* transcription reaction in the presence of cap analog.

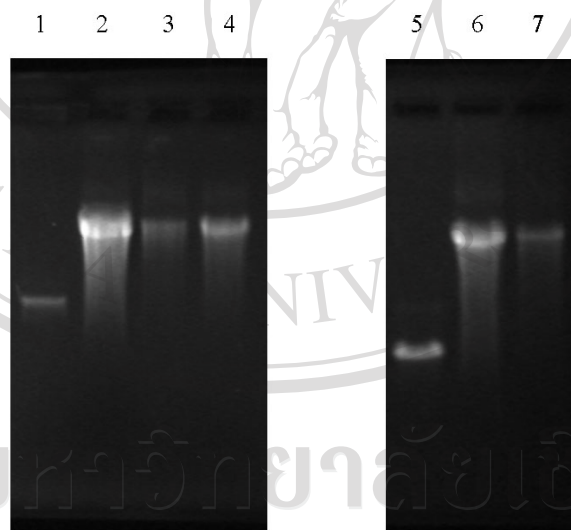


**Figure 20.** Agarose gel electrophoresis of the *in vitro* transcription products. The *in vitro* transcription products were denatured by heating and subjected to electrophoresis in a denaturing 0.7% agarose gel. The gel was stained with ethidium bromide and visualized under the UV light. Lanes 1 and 5, a positive RNA control, lanes 2 and 6, pBK(S1SP6-10723)Nde(+); lane 3, pBK(S1SP6-10723)pr(+6,-2)P10,13+; lane 4, pBK(S1SP6-10723)pr(+6,-2)P8,10+; lane 7, pBK(S1SP6-10723)pr(+6,-2)P8,13+.

When the products were electrophoresed in a denaturing agarose gel and stained with ethidium bromide, a major high molecular weight band and a slight smear were observed (Figure 20).

### 2.1.5 Generation of mutant dengue viruses by Lipofectin-mediated transfection

In the generation of mutant dengue viruses, ten  $\mu\text{l}$  of the *in vitro* transcripts were transfected into C6/36 cells by employing Lipofectin as the transfecting reagent. Transcripts of the full-length cDNA clone of strain 16681 served as a positive control. Following transfection, culture supernatants were collected at 0, 4, 7, 11 and 14 day after transfection and subjected to dot blot analysis. Two  $\mu\text{l}$  of the culture supernatants were dotted onto a nitrocellulose membrane and air dried. The membrane was blocked with 5% skimmed milk and then reacted sequentially with 4G2, an anti-flavivirus E antibody, and alkaline phosphatase-conjugated goat anti-mouse IgG antibody. With the use of NBT-BCIP, the presence of the E protein was indicated by the appearance of dark purple color (Figure 21)

In the dot blot analysis, the positive control, strain 16681 with an infectious virus titer of about  $10^7$  FFU/ml, displayed a dark purple color, which was reduced with sequential dilutions of the sample. The negative control, culture media of uninfected C6/36 cells, showed a very weak signal. Under the same conditions, the culture supernatants of C6/36 that had been transfected with capped *in vitro* transcripts of strain 16681Nde(+) became positive on day 7 after transfection and the signal intensity steadily increased on days 11, and 14 after transfection. Similar results, although with less signal intensity, were detected with culture supernatants of C6/36 transfected with *in vitro* transcripts of pBK(S1SP6-10723)pr(+6,-2)P10,13+ and pBK(S1SP6-10723)pr(+6,-2)P8,13+. In an exceptional case, the positive signal was observed on days 11 and 14, but not day 7, after transfection with the transcripts of pBK(S1SP6-10723)pr(+6,-2)P8,13+.

These results indicated that dengue E protein was present in the culture supernatants of C6/36 cells transfected with the capped RNA transcripts of the parental as well as the three mutant full-length cDNA clones. An increase in the signal intensity in the late period of transfection suggested that active virus replication

had taken place in the transfected cell culture. However, it was not yet clear whether infectious viruses had been generated.

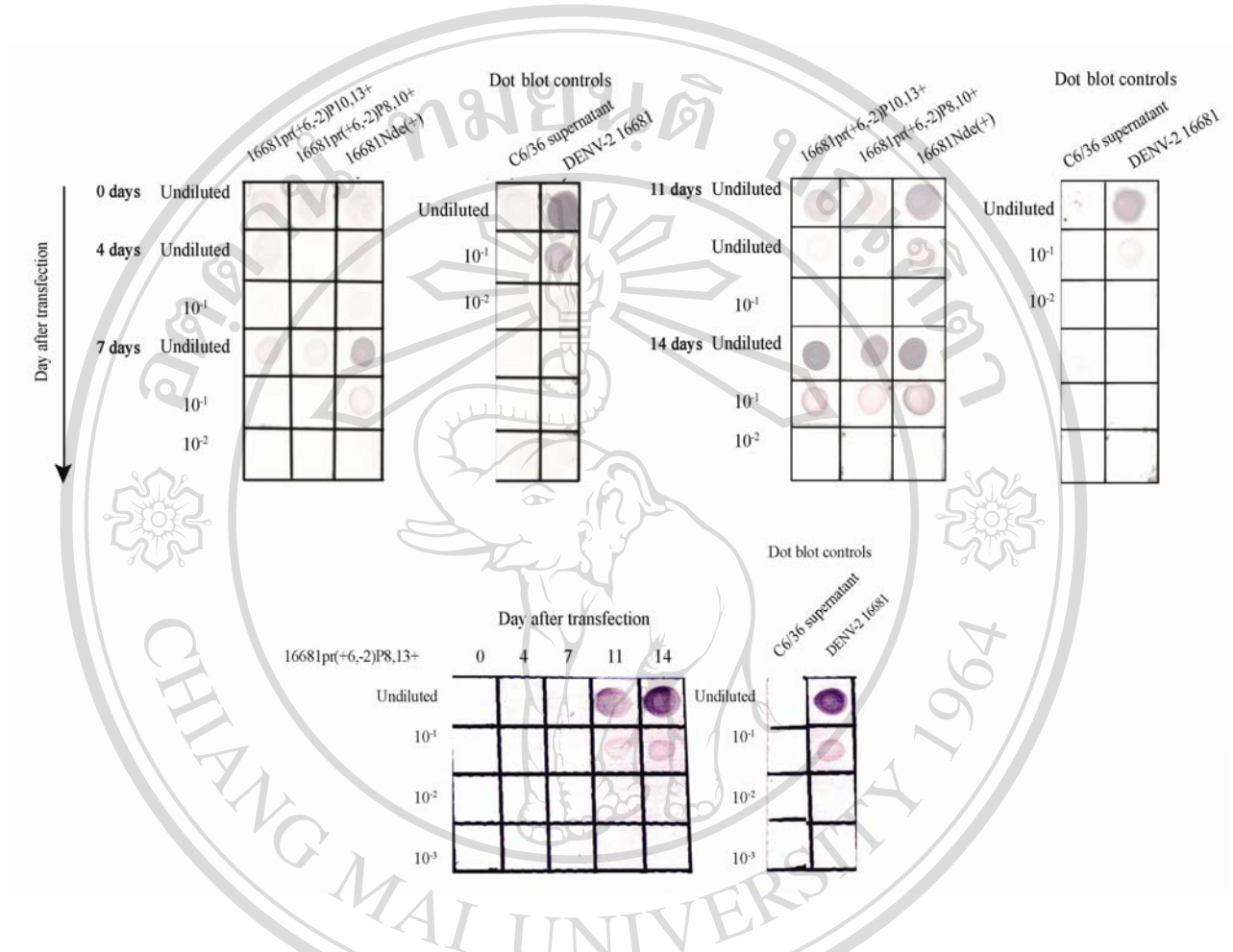


**Figure 21.** Detection of E protein in the culture supernatant by dot blot immunoassay.

Two  $\mu$ l of culture supernatant were dotted onto nitrocellulose membrane and then reacted with 4G2, an anti-flavivirus E protein monoclonal antibody, and an alkaline phosphatase-conjugated goat anti-mouse IgG antibody. The positive and negative controls were C6/36 culture media and the culture supernatant of strain 16681-infected cells, respectively. 16681Nde(+) indicates the positive control of transfection.

### 2.1.6 Determination of infectious virus titers in the culture supernatant of transfected C6/36 cells

The presence of infectious virus particles in the culture supernatant of transfected C6/36 cells was determined by subjecting the culture supernatants

collected on days 0, 4, 7, 11 and 14 after the transfection to the focus immunoassay titration. As shown in Figure 22, infectious viruses were detected on day 4 after transfection in all of the cultures. Subsequently, the virus titers rapidly increased, reaching the plateau of approximately  $10^7$  FFU/ml on day 14 after infection. During the two-week period of transfection, the infectious virus titers were generally higher in 16681Nde(+)-transfected culture than the others; this finding agreed well with the higher signal intensity of E protein in 16681Nde(+)-transfected culture detected with dot blot immunoassay.

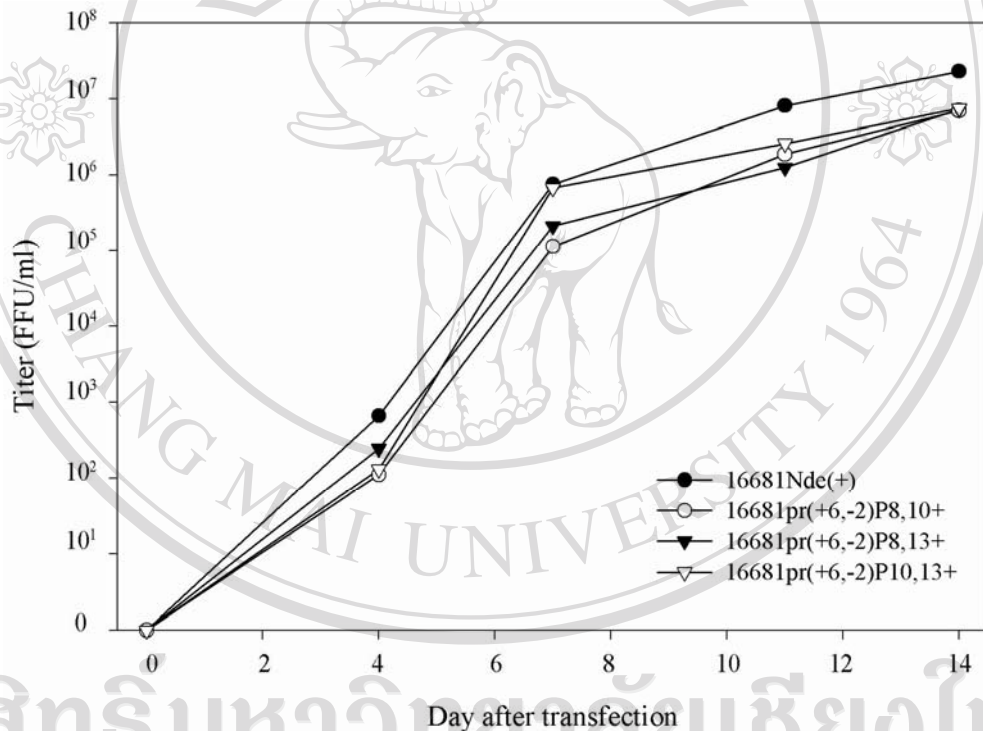


**Figure 22.** Production of infectious virus particles following the transfection of *in vitro* RNA transcripts into C6/36 cells. Culture media were collected on indicated days after transfection. Infectious virus titer was determined by using the focus immunoassay titration employing PS cells and expressed as FFU/ml.

These results showed that the mutant full-length cDNA clones were able to serve as the templates for the production of infectious RNA transcripts and subsequent generation of replicating viruses.

### 2.1.7 Expansion of mutant viruses

In order to obtain more viruses for subsequent studies, mutant viruses generated in the culture of RNA-transfected C6/36 cells were expanded in C6/36 cells at 29°C. Within a week after the infection, culture supernatants were collected and stored in the presence of 20% FBS. The titer of infectious viruses was determined by using the focus immunoassay titration and the average titers derived from three separate titration attempts are shown in Table 8. The average titers of all three mutant viruses exceeded the anticipated level of at least 10<sup>6</sup> FFU/ml.

**Table 8.** Virus expansion and titers of stock viruses

Virus	Expansion code	Day after Infection	Titer <sup>a</sup> (FFU/ml)
16681pr(+6,-2)P8,10+	C6-2/1(C6-1, D7, Tx.)	5	4.45 × 10 <sup>3</sup>
		7	9.36 × 10 <sup>5</sup>
16681pr(+6,-2)P8,10+	C6-2/2(C6-1, D7, Tx.)	5	9.03 × 10 <sup>5</sup>
		6	1.06 × 10 <sup>6</sup>
16681pr(+6,-2)P8,13+	C6-2(C6-1, D7, Tx.)	5	3.34 × 10 <sup>7</sup>
		7	1.71 × 10 <sup>6</sup>
16681pr(+6,-2)P10,13+	C6-2(C6-1, D7, Tx.)	4	2.30 × 10 <sup>5</sup>
		5	5.66 × 10 <sup>6</sup>

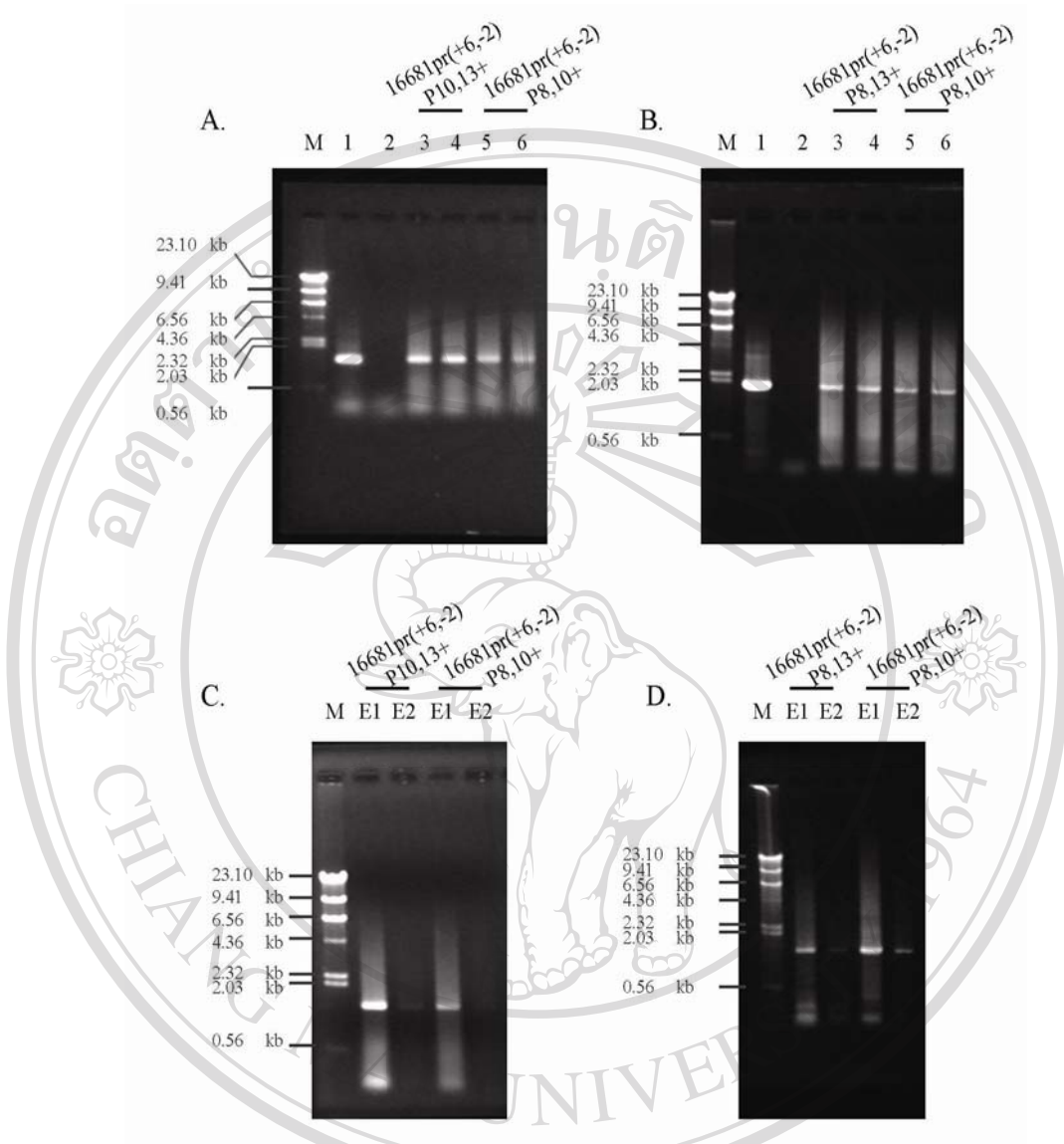


**Figure 23.** Electrophoretic analyses of the semi-nested PCR products. The prM coding region of the mutant virus was amplified and electrophoresed in 0.7% agarose gel. Panel A and B represent semi-nested PCR product: lane M, the DNA ladder; lane 1, a positive control reaction; lane 2, a negative control reaction; lanes 3 and 5, semi-nested PCR products generated with 1/100 dilution of RT-PCR products; lanes 4 and 6, semi-nested PCR products generated with 1/1,000 dilution of RT-PCR products. Panel C and D, the semi-nested PCR products were pooled and purified by gel extraction kit prior to electrophoresis: E1, purified PCR products from the first elution; E2, purified PCR products from the second elution. The sizes in kb of the  $\lambda$  DNA Hind III-digested fragments are on the left.

### 2.1.8 Verification of the pr-M junction mutations

The presence of intended double substitution mutation in the expanded virus stocks was verified by nucleotide sequence analysis. Genomic RNA was extracted from the three mutant virus preparations and used as template in RT-PCR.

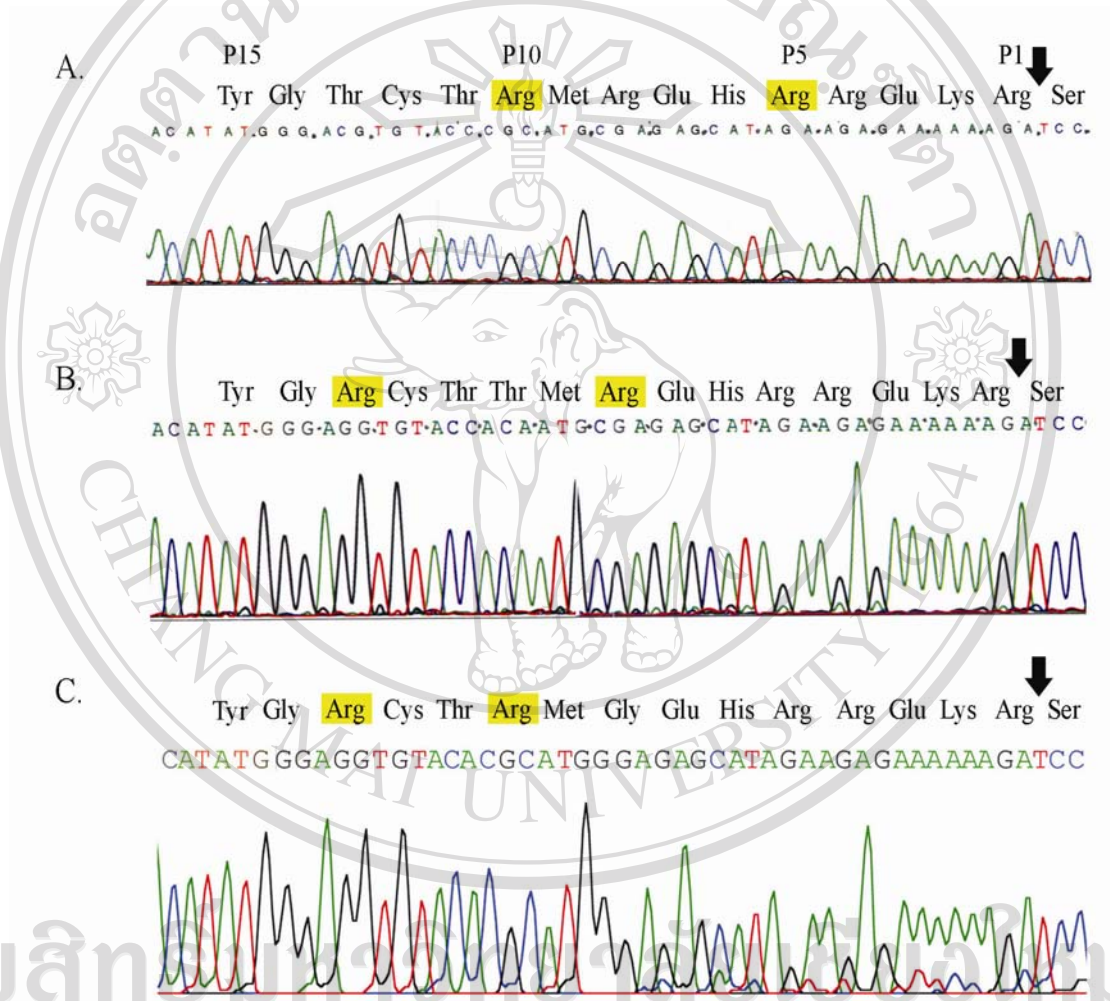


**Figure 24.** Nucleotide sequence of the prM coding region of pr-M junction double mutant viruses. The products of semi-nested PCR containing the entire prM coding region were employed in the sequencing reaction with the primer S350. Only the pr-M junction sequence is shown. The yellow highlights represent the intended arginine substitutions. Arrow indicates the pr-M junction. A, 16681pr(+6,-2)P8,10+; B, 16681pr(+6,-2)P8,13+, and C, 16681pr(+6,-2)P10,13+.

An entire prM coding region was further amplified by semi-nested PCR and the expected 1.3 kb PCR products were separated by electrophoresis in 0.7% agarose gel and purified (Figure 23). Analysis of the nucleotide sequence of these semi-nested PCR products revealed that the intended mutations of the pr-M junction were present in the mutant virus stock preparations (Figure.24). Additional mutation was not detected in the prM coding region. This result also indicated that the introduced mutated sequences were stable during the passage of viruses in C6/36 cells.

### 2.1.9 Reduction of focus size in the pr-M junction double mutant viruses

In a previous study, a pr-M junction chimeric virus, JEVpr/16681, was shown to exhibit a delay in particle export as well as the reduction in focus size during its replication in PS cells (Keelapang et. al., 2004). From an earlier experiment in this study, 16681pr(+7,-2), which shared arginine at P8, P10, and P13 at the pr-M cleavage junction with JEVpr/16681, also showed a delayed particle export and the reduction of focus size (Songjaeng, 2004). In an attempt to assess whether a combination of arginine at two of the three positions are responsible for these phenotypic changes, a 4-step peroxidase-anti-peroxidase immunostaining method was employed to determine the focus size of the three double mutant viruses, 16681pr(+6,-2)P8,10+, 16681pr(+6,-2)P8,13+ and 16681pr(+6,-2)P10,13+, with 16681Nde(+) and JEVpr/16681 serving as the controls. In this assay, dengue virus-infected cells were stained brown, especially in the perinuclear region (Figure 25). The numbers of infected cells in each cluster were counted and the arithmetic means derived from 40 foci or more was calculated and expressed as infected cells/focus.

For 16681Nde(+), the infected foci were generally large with the means  $\pm$  SD of  $240.3 \pm 75.43$  (SD) (Figure 26). As reported previously, JEVpr/16681 displayed very small foci with the focus size of  $24.1 \pm 10.53$  cells per focus; the reduction in focus size in JEVpr/16681 was about 89.9% (9.8 folds) when compared with 16681Nde(+). Under the same conditions, the reduction in focus size was observed in only two pr-M junction double mutant viruses: 16681pr(+6,-2)P8,10+ ( $55.4 \pm 24.99$  cell per focus, 76.9 % reduction, 4.3 folds) and 16681pr(+6,-2)P8,13+ ( $195.1 \pm 98.29$  cells per focus, 18.8 % reduction, 1.2 fold). The differences in the

focus size between these two mutants and 16681Nde(+) was statistically significant ( $P < 0.05$ ) when determined by the t-test. In contrast, the mean focus size of 16681pr(+6,-2)P10,13+ ( $283.58 \pm 128.41$  cells per focus) was slightly larger than that of 16681Nde(+) although this difference was not statistically significant (Figure 26).

These results indicated that the two combinations of double arginine substitution at P8 and P10 as well as P8 and P13 of the pr-M cleavage junction of strain 16681 resulted in the reduction of focus size during virus replication in PS cells. Alternatively, only the arginine substitution at P8 negatively affected the focus size whereas the presence of arginine at P10 and P13 did not influence the focus size. The second possible explanation may be confirmed by generating the P8 single arginine substitution mutant virus and determining its focus size.

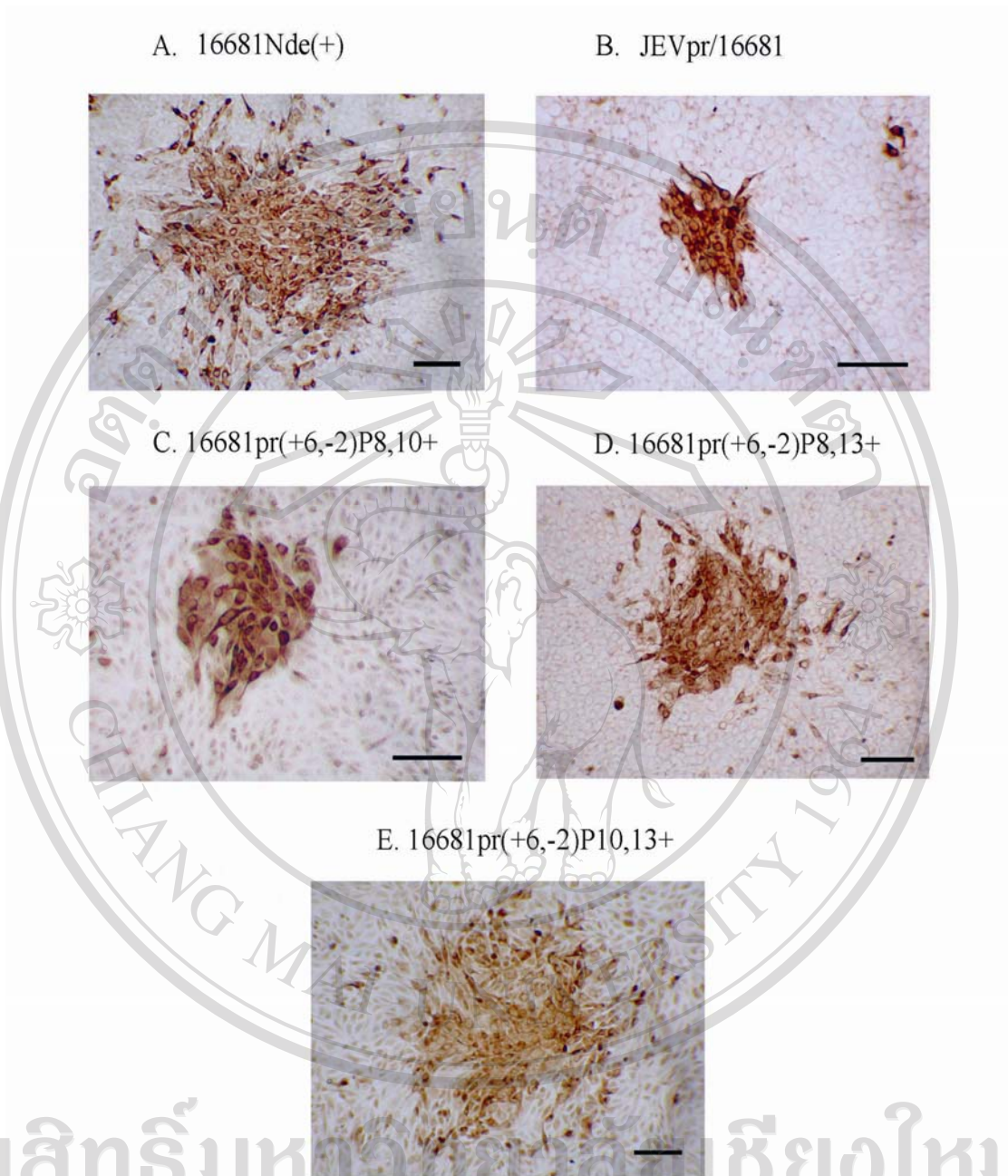


**Figure 25.** Alteration of focus size of pr-M junction double mutant viruses. PS cell monolayers were infected with each virus for three days under the methylcellulose overlayer, fixed, permeabilized, and then stained for the presence of E protein by a 4-step immunoassay. The scale bars represented 100  $\mu\text{m}$ .

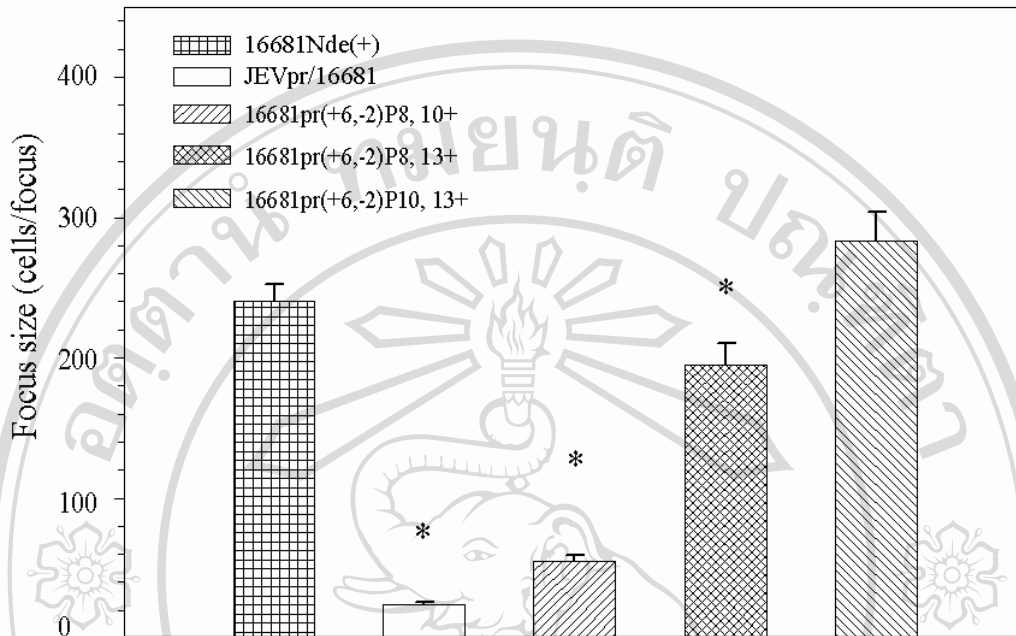


**Figure 26.** Focus size of dengue virus serotype 2 strain 16681Nde(+), JEVpr/16681 and double mutant viruses. PS cells were infected with each virus for three days under the methylcellulose overlay, fixed, permeabilized, and then stained for the presence of E protein by a 4-step immunostaining assay. The mean number of infected cells/focus was determined from 40 separated foci. Asterisk indicates statistically significant differences ( $P < 0.05$ ) between the mutant viruses and strain 16681Nde(+) as determined by using t-test.

## 2.2 Alteration of export in the pr-M junction mutant viruses

In an attempt to assess whether a combination of arginine at two of the three positions (P8, P10 and P13) of the pr-M junction are responsible for the delay in virus export in JEVpr/16681, a single-step kinetics experiment was employed. The three double mutant viruses, 16681pr(+6,-2)P8,10+, 16681pr(+6,-2)P8,13+ and 16681pr(+6,-2)P10,13+ were assessed in parallel with 16681Nde(+) and JEVpr/16681, which

served as the controls. The results of the single-step kinetics study were shown in Figure 27. As shown in the earlier experiments, changes in the titer of cell-associated viruses were comparable for strain 16681Nde(+), JEVpr/16681 and 16681pr(+7,-2) whereas the titers of extracellular virus were much lower with JEVpr/16681 and 16681pr(+7,-2) than 16681Nde(+). Similar results were observed with 16681pr(+6,-2)P8,10+ and 16681pr(+6,-2)P10,13+ although the reductions in the extracellular virus titers of these two mutant viruses were not as pronounced as those of JEVpr/16681 and 16681pr(+7,-2). In contrast, the extracellular titers of 16681pr(+6,-2)P8,13+ were indistinguishable from that of 16681Nde(+). Again, these results suggested that the combination of two arginine substitutions at P8 and P10 as well as P10 and P13, or a single arginine substitution at P10 is the cause a delayed export of JEVpr/16681 particles.

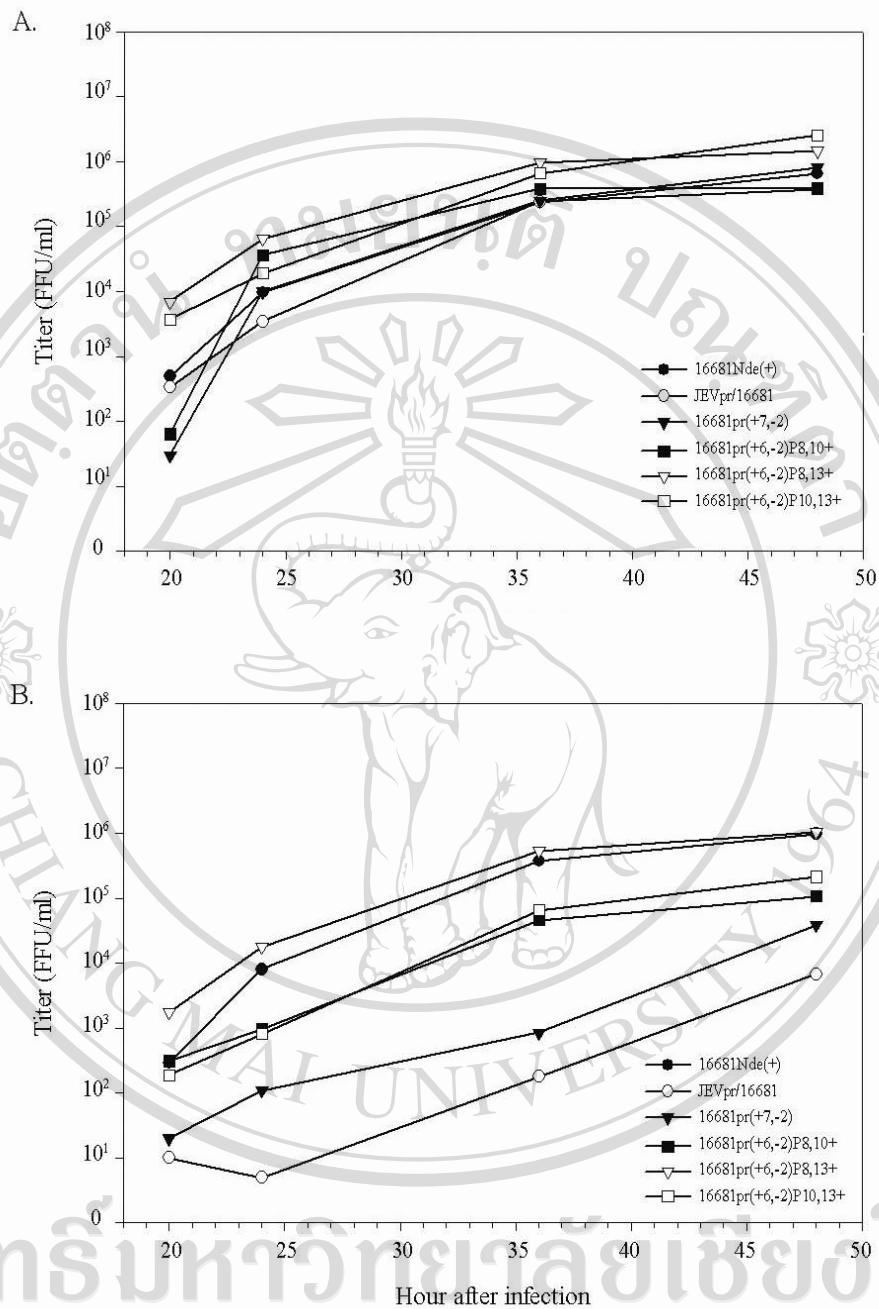


**Figure 27.** Single-step kinetic replication of the pr-M junction double mutant viruses. Changes in the infectious virus titer are shown separately for the cell-associated virus (A) and extracellular virus (B).